

Nitrogen and oxygen availabilities control water column nitrous oxide production during seasonal anoxia in the Chesapeake Bay

Qixing Ji¹, Claudia Frey¹, Xin Sun¹, Melanie Jackson², Yea-Shine Lee¹, Amal Jayakumar¹, Jeffrey C. Cornwell² and Bess B. Ward¹

¹Department of Geosciences, Princeton University, Princeton, 08544, New Jersey, USA

²Horn Point Laboratory, University of Maryland Center for Environmental Science, Cambridge, 21613, Maryland, USA

Correspondence to: Qixing Ji (qji@princeton.edu)

Abstract. Nitrous oxide (N₂O) is a greenhouse gas and an ozone depletion agent. [Estuaries that are subject to seasonal anoxia are generally regarded as N₂O sources.](#) However, insufficient understanding of the environmental controls on N₂O production results in large uncertainty about the estuarine contribution to the global N₂O budget. [Incubation experiments with nitrogen stable isotope tracer were used to investigate the geochemical factors controlling N₂O production from denitrification in the Chesapeake Bay,](#) the largest estuary in North America. The highest potential rates of water column N₂O production via denitrification ($7.5 \pm 1.2 \text{ nmol-N L}^{-1} \text{ hr}^{-1}$) were detected during summer anoxia, during which oxidized nitrogen species (nitrate and nitrite) were absent from the water column. At the top of the anoxic layer, N₂O production from denitrification was stimulated by addition of nitrate and nitrite. The relative contribution of nitrate and nitrite to N₂O production was positively correlated with the ratio of nitrate to nitrite concentrations. Increased oxygen availability, up to $7 \text{ } \mu\text{mol L}^{-1}$ oxygen, inhibited both N₂O production and the reduction of nitrate to nitrite. In spring, high oxygen and low abundance of denitrifying microbes resulted in undetectable N₂O production from denitrification. Thus, decreasing the nitrogen input into the Chesapeake Bay has two potential impacts on the N₂O production: a lower availability of nitrogen substrates may mitigate short-term N₂O emissions during summer anoxia, and in the long-run (time scale of years), eutrophication will be alleviated and subsequent re-oxygenation of the bay will further inhibit N₂O production.

1 Introduction

Nitrous oxide (N₂O) is a strong greenhouse gas with 298-fold higher global warming potential per mole than that of carbon dioxide. N₂O is also a catalyst of ozone depletion in the stratosphere. Since the Industrial Revolution, the N₂O atmospheric concentration has been increasing at an unprecedented rate, and the current concentration is the highest in the last 800,000 years of Earth's history (Schilt et al., 2010). The contribution of N₂O emissions to global warming and ozone depletion will increase because N₂O is not as strictly regulated as are CO₂ and halocarbon compounds. With the successful mitigation of halocarbon compounds accomplished by the Montreal Protocol, N₂O is likely to be the single most important

29 anthropogenically emitted ozone-depleting agent in the 21st century (Ravishankara et al., 2009).

30 Microbial processes are responsible for the majority of N₂O production, both in natural and anthropogenically impacted
31 environments. These pathways include oxidative and reductive processes occurring at the full range of environmental oxygen
32 concentrations. In the presence of oxygen, N₂O can be produced as a by-product during autotrophic aerobic ammonium (NH₄⁺)
33 oxidation to nitrite (NO₂⁻) by bacteria (Arp and Stein, 2003) and archaea (Santoro et al., 2011). The production of N₂O can
34 also occur via NO₂⁻ reduction by nitrifying organisms, termed nitrifier denitrification. This process was demonstrated in
35 cultures (Poth and Focht, 1985; Frame and Casciotti, 2010), and in the water column of the subtropical North Pacific
36 Ocean (Wilson et al., 2014). Under low oxygen and anoxic conditions, denitrifying bacteria produce N₂O via enzyme-mediated
37 heterotrophic denitrification, which consists of the stepwise reduction of nitrate (NO₃⁻), NO₂⁻ and nitric oxide (NO), with
38 organic matter as the electron donor. The *nirS* gene that encodes the genetic material for nitrite reductase (the enzyme mediating
39 NO₂⁻ reduction to NO) is often used as a proxy for abundance and diversity of denitrifying bacteria, and is the gene in the
40 denitrification sequence that is most reliably associated with a complete denitrification pathway (Graf et al., 2014). N₂O is not
41 produced via anaerobic ammonium oxidation (anammox), another important nitrogen removal process in the natural
42 environment (Kartal et al., 2011).

43 The increase of atmospheric N₂O is attributed to intensification of human activities (e.g. fossil fuel combustion, fertilizer
44 application, human and animal waste disposal), which alter the microbial nitrogen cycle in the biosphere. Increased nitrogen
45 supply from fertilizer and atmospheric deposition causes increased N₂O emission not only from agricultural land, but also in
46 rivers, streams and coastal waters (Ciais et al., 2013; Thompson et al., 2014). Among these aquatic environments, intense N₂O
47 efflux originates from estuaries and associated river networks, which occupy 0.3% of global waters (Dürr et al., 2011) but
48 could contribute up to 10 % of anthropogenic fluxes (Seitzinger and Kroeze, 1998; Ciais et al., 2013). Being the largest estuary
49 in the North America, the Chesapeake Bay and its tributaries have experienced eutrophication and expansion of summertime
50 anoxia due to increased population, expansion of industrialization and land use changes since the 18th century (Cooper and
51 Brush, 1993; Boesch et al., 2001). The Chesapeake tributary is a source of N₂O (indicated by surface N₂O oversaturation) in
52 the summertime between June and September (Elkins et al., 1978; Kaplan et al., 1978; McElroy et al., 1978). The summertime
53 water column is characterized by strong oxygen gradients (equilibrium with atmosphere at the surface and complete anoxia

54 below ~ 10 m), depletion of NO_3^- and NO_2^- , and accumulation of NH_4^+ in the deep water (Lee et al., 2015b). Increased microbial
55 activities driving carbon assimilation and respiration have been demonstrated in the vicinity of the oxic-anoxic interface in the
56 water column (Lee et al., 2015a). However, the N_2O production pathway and the associated environmental controlling factors
57 have not been investigated in the Chesapeake Bay.

58 Here we report a pilot study using nitrogen stable isotope (^{15}N) incubation experiments to quantify N_2O production rates
59 and their dependence on the availabilities of oxygen, NO_3^- and NO_2^- in the Chesapeake Bay. Because seasonal anoxia occurs
60 at the study site in the central region of the Chesapeake Bay, reductive pathways of N_2O production (i.e. reduction of NO_3^- and
61 NO_2^-) are the main focus. Further understanding of the environmental controls on N_2O production in estuaries will facilitate
62 the design of effective environmental engineering projects to mitigate N_2O emission.

63 **2 Methods**

64 **2.1 Sample acquisition and processing**

65 Sampling and incubation experiments were carried out on July 19, 2016, November 17, 2016 and May 3, 2017,
66 corresponding to typical conditions of summer, autumn and spring, respectively. Samples were collected at 38.55 °N, 76.43
67 °W (bottom depth 26.5 m) close to the mouth of the Choptank River in the central region of the Chesapeake Bay. Conductivity-
68 temperature-depth and dissolved oxygen ($[\text{O}_2]$) were measured with a YSI sonde package (Model 600XLM with a 650 MDS
69 display logger) equipped with a diaphragm pump which was deployed for water sampling. The oxygen sensor had a detection
70 limit of ~ 5 $\mu\text{mol L}^{-1}$. Samples for NO_2^- and NO_3^- concentration measurements were filtered (0.22 μm poresize, Sterivex-GP,
71 EMD Millipore) and frozen at -80 °C until analysis. Discrete samples for N_2O concentration were collected directly from the
72 pump outlet into the bottom of acid washed, 60 mL glass serum bottles (Catalog # 223745, Wheaton, Millville, NJ). Bottles
73 were sealed with butyl rubber stoppers (Catalog # W224100-202, Wheaton, Millville, NJ) and aluminium rings while
74 submerged under water pumped from depth to avoid atmospheric N_2O and oxygen contamination. Samples for characterizing
75 N_2O concentration profile were preserved immediately after filling by injecting 0.1 mL saturated HgCl_2 . Samples for N_2O
76 incubation experiments (section 2.2) were acquired from 12 m, 17 m and 19.5 m during July 2016, November 2016 and May
77 2017, respectively, and sealed the same way as described above for discrete N_2O concentration samples, and stored in the dark

78 at 4 °C without adding HgCl₂. Samples for denitrifying *nirS* gene abundance were collected at 14, 17 and 19.5 m by filtering
79 600mL - 2000mL of water through 0.22 µm filter (Sterivex-GP, EMD Millipore) and frozen at -80 °C until DNA extraction
80 and analysis.

81 Samples for total dissolved inorganic carbon (DIC=[H₂CO₃]+[HCO₃⁻]+[CO₃²⁻]) and community respiration rates were
82 collected only in July 2016. The DIC samples were preserved with mercuric chloride (HgCl₂) for initial conditions, while
83 biochemical oxygen demand (BOD) bottles were incubated in a temperature-controlled environmental chamber (±1 °C of in
84 situ water temperatures). After 24 hours, samples were siphoned from the vials, preserved with HgCl₂, and respiration rates
85 were determined as the difference in DIC between initial and final samples divided by 24 hours (Lee et al., 2015b).

86 2.2 ¹⁵N incubation experiments for N₂O production

87 Within 3 hours of sampling, incubation experiments were initiated at the Horn Point Laboratory, Cambridge, Maryland.
88 Samples were divided into three sets for control, nitrogen manipulation and oxygen manipulation experiments.

89 Control experiment: The control experiment was conducted in July 2016, November 2016 and May 2017. A small (3
90 mL) headspace was created in the serum bottles, which were subsequently flushed with helium for 10 minutes to minimize
91 oxygen contamination from sampling and transportation. Two suites of ¹⁵N tracer solutions (¹⁵NO₂⁻ plus ¹⁴NO₃⁻, ¹⁵NO₃⁻ plus
92 ¹⁴NO₂⁻, 0.1mL) were injected to achieve final concentrations of 5 µmol L⁻¹ NO₂⁻ and NO₃⁻ (see conditions for experiment 1-A
93 and 1-B, 4-A and 4-B, 6-A and 6-B in Table 1). Tracer solutions were made from deionized water, and were flushed with
94 helium prior to addition to incubation experiments. In order to have enough mass to detect N₂O production, ~1.2 nmol of
95 natural abundance N₂O was injected to each bottle, reaching a concentration of ~ 20 nmol L⁻¹ in the water phase (calculated
96 equilibrium concentration according to Weiss and Price (1980) with 3 mL headspace and 57 mL water). Initial conditions (one
97 bottle for each time course) were sampled within 30 minutes of tracer addition by injecting 0.1 mL saturated HgCl₂. Incubations
98 lasted ~ 2 hours at *in situ* temperature (±0.5 °C), during which duplicate bottles were preserved with saturated HgCl₂ solution
99 every 40 to 60 minutes, totalling seven bottles over four time points, including the initial for a time course analysis.

100 Dissolved inorganic nitrogen (DIN) manipulation: The DIN manipulation experiment was conducted only in July 2016
101 because NO₂⁻ and NO₃⁻ were absent from the water column (see section 3.1). A 3 mL headspace was created before flushing
102 with helium for 10 min to establish anoxic condition. Then, ~ 1.2 nmol N₂O was injected to reach a concentration of ~20 nmol

103 L⁻¹ in the water phase. Two suites of ¹⁵N tracer solutions (¹⁵NO₂⁻ plus ¹⁴NO₃⁻, ¹⁵NO₃⁻ plus ¹⁴NO₂⁻, 0.1 mL of total volume of
104 tracer addition) were injected to designated bottles to achieve ratios of NO₂⁻ : NO₃⁻ ≈ 1:10, 1:3, 3:1 and 10:1, with ¹⁵N fraction
105 labelled between 0.016 and 0.16 (Table 1, experiment 2-A to 2-H). This allowed simultaneous detection of N₂O production
106 from NO₂⁻ and NO₃⁻ at different ratios of NO₂⁻ to NO₃⁻ concentration. Incubations lasted ~ 2 hours with the same sampling
107 strategy as the control experiment.

108 Oxygen manipulation: The oxygen manipulation experiment was conducted in July 2016 and November 2016.
109 Headspace (3 – 8 mL) was created before flushing with helium for 10 minutes. Oxygen-saturated site water was made by air-
110 equilibration at *in situ* temperature. To achieve different oxygen levels, 0.2, 0.5, 1.0, 2.0 or 5.0 mL of oxygen-saturated site
111 water was injected. With a final volume of ~3 mL of headspace during the course of the incubation, the oxygen concentrations
112 in the water phase were 0.3 to 6.4 μmol L⁻¹ in July 2016 (Table 1, experiment 3-A – 3-J), and were 0.2 to 7.3 μmol L⁻¹ in
113 November 2016 (Table 1, experiment 5-A – 5-J) after the calculated equilibration between headspace and water (Garcia and
114 Gordon, 1992). In addition, an optical sensor was used to measure oxygen concentrations directly in a parallel experimental
115 setup and the agreement between calculated target concentration and measured concentration was excellent (data not shown).
116 After oxygen adjustment, ~1.2 nmol N₂O was injected into each bottle, and two suites of ¹⁵N tracer solutions (¹⁵NO₂⁻ plus
117 ¹⁴NO₃⁻, ¹⁵NO₃⁻ plus ¹⁴NO₂⁻, 0.1mL) were injected to achieve final concentration of 5 μmol L⁻¹ NO₂⁻ and NO₃⁻. The ¹⁵N fraction
118 for NO₂⁻ or NO₃⁻ during the incubation experiments are shown in Table 1. Incubations lasted ~ 2 hours with the same sampling
119 strategy as the control experiment.

120 **2.3 Analytical procedures**

121 For water column nutrients, dissolved NO₂⁻ was measured using a colorimetric method (Hansen and Koroleff, 2007) and
122 NO₃⁻ + NO₂⁻ was measured using a hot (90 °C) acidified vanadium (III) reduction column coupled to a chemiluminescence
123 NO/NO_x Analyzer (Teledyne API, San Diego, CA) (Garside, 1982; Braman and Hendrix, 1989). DIC was measured with an
124 automated infrared analyzer (Apollo SciTech, Newark, DE) as previously reported (Lee et al., 2015b). Preserved N₂O samples
125 were stored in the dark at room temperature (~22 °C) for less than three weeks before analysis. Dissolved N₂O was extracted
126 by flushing with helium for 40 min at a rate of 37 mL min⁻¹ (extraction efficiency 99 ± 2 %), and subsequently cryo-trapped
127 by liquid nitrogen and isolated from interfering compounds (H₂O, CO₂) by gas chromatography (Weigand et al., 2016). Pulses

128 of purified N₂O were injected into an isotope ratio mass spectrometer (Delta V^{Plus}, Thermo Fisher Scientific, Waltham, MA)
129 for mass (m/z = 44, 45, 46) and isotope ratio (m₁/m₂ = 45/44, 46/44) measurements. The amount of N₂O was calibrated with
130 standard N₂O vials, which were made by injecting 1, 2, or 5 nmol N₂O-N into 20 mL glass vials (Catalog # C4020-25, Thermo
131 Fisher Scientific, Waltham, MA).

132 After N₂O analysis, samples incubated with ¹⁵NO₃⁻ were also assayed for ¹⁵NO₂⁻ to determine rates of NO₃⁻ reduction.
133 Two millilitres of each sample were transferred from the 60-mL serum bottle to a 20-mL glass vial and then flushed with
134 helium for 10 min. Dissolved ¹⁵NO₂⁻ was converted to N₂O using the acetic acid-treated sodium azide solution for quantitative
135 conversion (McIlvin and Altabet, 2005). Resulting N₂O was measured for nitrogen isotope ratio (¹⁵N/¹⁴N) so as to determine
136 the ¹⁵N enrichment of NO₂⁻.

137 For the analysis of *nirS* gene abundance, DNA extraction and qPCR for the *nirS* gene using SYBR Green were performed
138 as previously described (Jayakumar et al. 2009; 2013). Extracted DNA was quantified using PicoGreen fluorescence
139 (Molecular Probes, Eugene, OR) prior to the qPCR assay. Samples for qPCR were run in triplicates including a no-template
140 control, a no-Primer control and 5 different dilutions of a *nirS* standard. Threshold cycle (Ct) values were obtained using
141 automatic analysis settings of the quantitative PCR and further used to calculate the gene copy numbers as described in
142 Jayakumar et al. (2013).

143 2.4 Data analysis

144 N₂O concentration was calculated from the amount of N₂O detected by mass spectrometry divided by the volume of
145 water in the serum bottles. N₂O production (*R*) was calculated from the progressive increase in ⁴⁵N₂O and ⁴⁶N₂O concentrations
146 in each serum bottle over the time course experiments.

$$147 \quad R = \frac{1}{F} \times \left(\frac{d^{45}\text{N}_2\text{O}}{dt} + 2 \times \frac{d^{46}\text{N}_2\text{O}}{dt} \right) \quad (1)$$

148 where $d^{45}\text{N}_2\text{O}/dt$ and $d^{46}\text{N}_2\text{O}/dt$ represent the production rates (nmol-N L⁻¹ hr⁻¹) of mass 45 and 46 N₂O during incubation. *F*
149 represents the ¹⁵N fraction in the initial substrate (NO₂⁻ or NO₃⁻). Rates were considered significant based on the linear
150 regression of the time course data having *p* < 0.05 (*n*=7, student *t*-test). The detection limit for N₂O production was 0.002
151 nmol-N L⁻¹ hr⁻¹. The ¹⁵N incubation experiments can identify the pathway but cannot distinguish the relative contributions of

152 two or more functioning microbial groups to a single N₂O production pathway (i.e. N₂O production via NO₂⁻ reduction by
153 nitrifier denitrification and/or heterotrophic denitrification).

154 The rate of NO₃⁻ reduction to NO₂⁻ was calculated as

$$155 \text{ NO}_2^- \text{ production} = (d^{15}\text{NO}_2^-/dt) / F \quad (2)$$

156 where $d^{15}\text{NO}_2^-/dt$ represents the production rate of ¹⁵NO₂⁻ (nmol-N L⁻¹ hr⁻¹). *F* represents initial ¹⁵N enrichment of substrate
157 NO₃⁻. Rates were considered significant based on linear regression of the time course data having p<0.05 (student's t-test).

158 The detection limit for NO₂⁻ production was 0.05 nmol-N L⁻¹ hr⁻¹.

159

160 **3 Results and discussion**

161 **3.1 Water column features**

162 The physical and chemical properties of the water column in central Chesapeake Bay showed seasonal variation (Fig. 1).
163 Temperature and salinity differed among the three seasons but were essentially constant in the top 7 m of the water column on
164 the three sampling dates. In July, the water column was stratified because of lower salinity (~ 16 PSU) and higher temperature
165 (~ 28.5 °C) in the top ~ 10 m resulting in a pronounced halocline and thermocline (Fig. 1a and 1b). Less pronounced
166 stratification in May and November was due to a weaker temperature difference between the top 10 m and below. The July
167 oxygen profile showed a significant concentration decrease between 3 to 10 m (Fig. 1c), with a sharp oxycline (~ 30 μmol L⁻¹
168 m⁻¹). Below 10 m, the oxygen concentration was below detection of the sensor (~ 5 μmol L⁻¹) and was likely anoxic. **The water**
169 **samples were free of any hydrogen sulphide odor, so we conclude that sulphide was either absent or was present at very low**
170 **level (< 1 μmol L⁻¹).** No anoxic layer was observed in May and November (Fig. 1c), and previous studies showed that the
171 water column of the Chesapeake Bay was reoxygenated following summertime anoxia during winter and spring (Lee et al.,
172 2015a).

173 The surface N₂O saturation concentrations in July, November and May were 6.6, 10.4 and 12.0 nmol L⁻¹, respectively.
174 In July, N₂O concentration was close to air-saturation level (6.6 nmol L⁻¹) at the surface layer. In the low oxygen layer (below
175 12 m), N₂O was apparently undersaturated (2.0 – 3.7 nmol L⁻¹, 20 – 50 % air-saturation, Fig. 1d). In November, the surface
176 N₂O concentration was slightly oversaturated (11.3 nmol L⁻¹, 108 % air-saturation). N₂O concentrations at depth were

177 oversaturated; the concentrations varied between 11.0 and 11.5 nmol L⁻¹, corresponding to 109 – 115 % air-saturation. In May,
178 both the surface and water column N₂O concentrations were air-undersaturated; the surface concentration was 9.1 nmol L⁻¹,
179 76 % air-saturation; concentrations between 8 and 17 m ranged from 9.4 to 11.0 nmol L⁻¹, corresponding to 82 – 97 % air-
180 saturation. As the surface and water column N₂O saturation levels vary greatly between seasons; the assessment of the N₂O
181 dynamics of the Chesapeake Bay requires expanding the temporal and spatial coverage of the field sampling. In the following,
182 we focus on N₂O production and its environmental controlling factors.

183 The concentrations of NO₃⁻ and NO₂⁻ (Fig. 1e and 1f) in July were below 0.02 μmol L⁻¹ within the sampling depth interval
184 (top 17 m of water column). Measureable levels of NO₃⁻ and NO₂⁻ species were found in May and November. The surface
185 concentrations of NO₃⁻ and NO₂⁻ in May were 20 and 0.5 μmol L⁻¹, respectively; and the concentrations decreased with depth.
186 In November, NO₃⁻ and NO₂⁻ were depleted at the surface (~ 3 m) and their concentrations increased with depth; at 17 m the
187 concentrations of NO₃⁻ and NO₂⁻ were 5.0 and 0.4 μmol L⁻¹, respectively. The increase of water column NO₃⁻ and NO₂⁻
188 concentrations in May and November can be attributed to increased runoff from the anthropogenically influenced watershed.
189 Water column depletion of NO₃⁻ and NO₂⁻ in the summer is the result of denitrification (Baird et al., 1995; Boynton et al.,
190 1995), which indicates potential water column N₂O production via denitrification (discussed in section 3.2).

191 As a proxy for the size of the denitrifying community, the abundance of the *nirS* gene was $(5.91 \pm 0.1) \times 10^4$ copy mL⁻¹
192 at 14 m in July, which was the highest among the three sampling trips (Fig. 1g). Lowest *nirS* gene abundance $(9.1 \pm 1.3) \times 10^3$
193 copy mL⁻¹ was observed in May at 19.5 m. The abundance of *nirS* was measured only at the depths at which incubations were
194 performed, and the *nirS* abundance increased with increasing rates of N₂O production (see section 3.2). In July 2016, water
195 column DIC concentrations ranged from 1,377 to 1,831 μmol L⁻¹, with the highest concentrations below 10 m. Average
196 community respiration rates at 3 m and 14 m depth were 2.01 and 0.63 μmol L⁻¹ hr⁻¹, respectively.

197 **3.2 Active water column N₂O production**

198 The anoxic control experiment (anoxic condition with 5 μmol L⁻¹ ¹⁵NO₂⁻ or ¹⁵NO₃⁻) was used to demonstrate active N₂O
199 production: In July 2016, at the top of anoxic layer (~ 12.3 m), rates of N₂O production from NO₂⁻ and NO₃⁻ reduction were
200 5.42 ± 0.35 and 2.04 ± 0.86 nmol-N L⁻¹ hr⁻¹, respectively (Fig. 2). In November 2016, at 17 m within the oxygenated water
201 column ([O₂] > 180 μmol L⁻¹), rates of N₂O production were 0.33 ± 0.01 and 0.95 ± 0.35 nmol-N L⁻¹ hr⁻¹, respectively. In May

202 2017, no N₂O production was detected at 19.5 m.

203 The total N₂O production rate of $7.5 \pm 1.2 \text{ nmol-N L}^{-1} \text{ hr}^{-1}$ in July 2016 is lower than the measurements (18 – 77 nmol-N
204 L⁻¹ hr⁻¹) made 40 years ago in the Potomac River (McElroy et al., 1978), a tributary to the Chesapeake Bay. This difference
205 could be due to much higher water column nutrients in the Potomac River (NO₂⁻ plus NO₃⁻ concentration > 30 μmol L⁻¹) at
206 that time, and presumably denser microbial populations because of sediment resuspension (4 – 10 m water depth). With added
207 substrates (NO₂⁻ and NO₃⁻) being more than an order of magnitude higher than *in situ* levels in July 2016, and the anoxic
208 conditions being used in the November 2016 experiments (*in situ* [O₂] > 180 μmol L⁻¹), N₂O production rates reported here
209 are potential rates, which nevertheless highlight the potential for N₂O production in anoxic waters responding rapidly (within
210 hours) to pulses of NO₂⁻ or NO₃⁻.

211 Based on the *nirS* gene abundance, the denitrifying population was more abundant in July than in November, and was
212 the smallest in May in the lower water column (14 – 19.5 m) of the Chesapeake Bay (Fig. 1g). In July the highest N₂O
213 production rates from denitrification co-occurred with the highest *nirS* abundances (Fig. 2). While the water column oxygen
214 in November was > 180 μmol L⁻¹, the *nirS* gene abundance supported potential denitrification at a N₂O production rate of 1.28
215 $\pm 0.35 \text{ nmol-N L}^{-1} \text{ hr}^{-1}$ in anoxic incubation experiments. In May when hypoxic conditions had not yet developed, reduction
216 of NO₂⁻ or NO₃⁻ to N₂O did not occur, and the *nirS* abundance ($9.1 \times 10^3 \text{ copies mL}^{-1}$) was the lowest among three seasons. It
217 is likely that the denitrifying community did not recover from oxygen inhibition during the 2-hour anoxic incubation. A
218 metatranscriptome analysis showed that the transcript ratios for denitrification were the lowest in June before the onset of
219 hypoxia, and highest ratios in August when anoxia was most pronounced (Eggleston et al., 2015).

220 **3.3 N₂O production pathways regulated by availability of nitrogen substrate**

221 The ratio of the rates of N₂O production from NO₂⁻ reduction vs. N₂O production from NO₃⁻ reduction positively
222 correlates with the ratio of NO₂⁻ : NO₃⁻ concentrations (Fig. 3). This suggests increasing NO₂⁻ or NO₃⁻ availability favours N₂O
223 production from the reduction of the respective substrate. At concentration ratios of NO₂⁻ : NO₃⁻ < 0.5, the ratios of rates were
224 similar to the concentration ratio, 0.3 ± 0.2 . At a concentration ratio of NO₂⁻ : NO₃⁻ = 1 : 1, the ratio of rates of N₂O production
225 from respective substrates measured from replicate experiments varied from 0.6 to 2.6. At NO₂⁻ : NO₃⁻ = 10, the ratio of rates

226 was greater than 10. Therefore, the primary nitrogen source of N₂O production via denitrification depends in part on the relative
227 availability of the substrate (NO₂⁻ or NO₃⁻).

228 As denitrification is a step-wise enzymatic reduction from NO₃⁻, NO₂⁻, NO, N₂O to N₂, the pathway can be somewhat
229 modular (Graf et al., 2014), i.e., many organisms possess only one or a few steps, rather than the complete pathway. In complete
230 denitrifiers (organisms capable of reducing NO₃⁻ to N₂), the degree to which intermediates (i.e. NO₂⁻) exchange across cellular
231 membranes with the ambient environment is unknown (Moir and Wood, 2001). We use data from the DIN manipulation
232 experiment (conducted in July 2016) to show that full exchange between intracellular and ambient NO₂⁻ during NO₃⁻ reduction
233 to N₂O is unlikely, as explained below.

234 The conditions and results from experiment 2-H (Table 1) were used because this experiment had the highest ambient
235 NO₂⁻ pool; an exchange between the pools could be easily detected. During NO₃⁻ reduction to N₂O, if denitrifiers reduce ¹⁵NO₃⁻
236 (total 1.2 μmol L⁻¹, ¹⁵N fraction labeled 0.16) to ¹⁵NO₂⁻ at maximal rate (0.2 μmol-N L⁻¹ hr⁻¹, see section 3.4) and the product
237 fully exchanges with the ambient ¹⁴NO₂⁻ (10 μmol L⁻¹, ¹⁵N fraction labeled 0.0037), after 2 hours, the ¹⁵N addition to the total
238 NO₂⁻ pool will be 0.064 μmol L⁻¹:

239 (Rate of NO₂⁻ production from NO₃⁻ × incubation time × initial fraction labelled of NO₃⁻)
240 = (0.2 μmol-N L⁻¹ hr⁻¹ × 2 hr × 0.16) = 0.064 μmol L⁻¹,

241 and the resulting ¹⁵N fraction (unitless) of NO₂⁻ will be 0.01:

242 (¹⁵N addition to NO₂⁻ + initial fraction labelled of NO₂⁻ × initial concentration of NO₂⁻) / (total concentration of NO₂⁻)
243 = (0.064 μmol L⁻¹ + 0.0037 × 10 μmol L⁻¹) / (10 + 0.064) μmol L⁻¹ ≈ 0.01.

244 Assuming 6 nmol-N L⁻¹ hr⁻¹ as the rate of N₂O production from NO₂⁻ reduction (the NO₂⁻ → N₂O rate shown in Fig. 3; ¹⁵N
245 fraction labeled of NO₂⁻ = 0.01), and the initial N₂O concentration as 20 nmol L⁻¹ (described in section 2.2; ¹⁵N fraction labeled
246 of N₂O = 0.0037), after 2 hours, the resulting ¹⁵N fraction of N₂O will be 0.0052:

247 ((¹⁵N fraction labelled of NO₂⁻ × rate of N₂O production from NO₂⁻ × incubation time) + (initial fraction labelled of N₂O × initial
248 concentration of N₂O × molar nitrogen in molar N₂O)) / ((rate of N₂O production from NO₂⁻ × incubation time) + (initial
249 concentration of N₂O × molar nitrogen in molar N₂O))
250 = ((0.01 × 6 nmol-N L⁻¹ hr⁻¹ × 2 hr) + (0.0037 × 20 nmol-N₂O L⁻¹ × 2N/N₂O)) / (6 × 2 + 20 × 2) nmol-N L⁻¹ = 0.0052

251 The calculated ^{15}N fraction of N_2O (0.0052) is much lower than the measured ^{15}N fraction of N_2O (> 0.02) in experiment 2H.
252 This means that full exchange of NO_2^- during NO_3^- reduction to N_2O , at maximum possible rates of NO_3^- reduction to NO_2^-
253 and N_2O , would yield a rate of N_2O production from NO_3^- much lower than observed in the experimental results. Thus, we
254 concluded that the intracellular exchange of NO_2^- during NO_3^- reduction to N_2O by the denitrifying community in Chesapeake
255 Bay is limited. Such a tight coupling among nitrate reduction, nitrite reduction and nitric oxide reduction suggests the co-
256 occurrence of the respective functional genes and enzymes in the cell of nitrate reducers. Both dissimilatory nitrate and nitrite
257 reducers are able to produce N_2O independently, so total N_2O production can be quantified accurately by separate measurement
258 of NO_3^- and NO_2^- reduction.

259 **3.4 Oxygen inhibits N_2O production by denitrification**

260 The sensitivities to increasing $[\text{O}_2]$ of NO_2^- reduction and NO_3^- reduction to N_2O were evaluated in samples from July
261 and November 2016 (Fig. 4). The control experiments (anoxic incubation, see Section 3.2) in July 2016 and November 2016
262 showed rates of N_2O production from denitrification of 7.5 ± 1.2 and 1.28 ± 0.35 $\text{nmol-N L}^{-1} \text{hr}^{-1}$, respectively. Increasing $[\text{O}_2]$
263 generally decreased N_2O production rates from denitrification. In July 2016, under $[\text{O}_2] = 0.3 \mu\text{mol L}^{-1}$, N_2O production from
264 NO_2^- reduction decreased from 5.4 to 2.5 $\text{nmol-N L}^{-1} \text{hr}^{-1}$, whereas the rate of NO_3^- reduction to N_2O increased from 2.0 to 3.5
265 $\text{nmol-N L}^{-1} \text{hr}^{-1}$. Further increase in $[\text{O}_2]$, up to $6.4 \mu\text{mol L}^{-1}$, did not fully inhibit N_2O production from NO_2^- reduction, the rate
266 of which was $0.08 \text{ nmol-N L}^{-1} \text{hr}^{-1}$. However, N_2O production from NO_3^- reduction was completely inhibited when $[\text{O}_2] > 0.6$
267 $\mu\text{mol L}^{-1}$ (Fig. 4a). In November 2016, increasing $[\text{O}_2]$ gradually decreased rates of NO_2^- reduction to N_2O ; no rates were
268 detected when $[\text{O}_2] > 2 \mu\text{mol L}^{-1}$. Rates of NO_3^- reduction to N_2O were not detected at $[\text{O}_2] > 0 \mu\text{mol L}^{-1}$ (Fig. 4b).

269 Rates of NO_3^- reduction to NO_2^- under increasing $[\text{O}_2]$ was also measured in July 2016 to supplement the sensitivity
270 analysis of denitrification to oxygen. The rate of NO_3^- reduction to NO_2^- was $100 \text{ nmol-N L}^{-1} \text{hr}^{-1}$ under anoxic condition. At
271 $[\text{O}_2] = 0.3 \mu\text{mol L}^{-1}$, the rate doubled, to $200 \text{ nmol-N L}^{-1} \text{hr}^{-1}$ (Fig. 4). Further increase of $[\text{O}_2]$ significantly decreased the rate
272 of NO_3^- reduction to NO_2^- . However, at $[\text{O}_2] = 6.4 \mu\text{mol L}^{-1}$ NO_3^- reduction to NO_2^- was still detectable at $0.82 \pm 0.06 \text{ nmol-N}$
273 $\text{L}^{-1} \text{hr}^{-1}$ (Fig. 5).

274 These results suggest that oxygenation of the water column in the Chesapeake Bay, even micro-molar level oxygen,
275 would significantly mitigate N₂O production from denitrification. Both July 2016 and November 2016 data showed the
276 difference in the effect of oxygen on N₂O production from NO₂⁻ vs. NO₃⁻ reduction. Samples from July 2016 showed 98% and
277 complete inhibition on N₂O production from NO₂⁻ and NO₃⁻ reduction at [O₂] = 6 μmol L⁻¹, respectively. The November 2016
278 samples showed 94 % and complete inhibition on N₂O production from NO₂⁻ and NO₃⁻ reduction at [O₂] = 0.4 μmol L⁻¹,
279 respectively. Furthermore, N₂O production in the Chesapeake Bay was likely attributed to both heterotrophic denitrification
280 and nitrifier denitrification. Studies have shown that both nitrifiers and denitrifiers are present in the Chesapeake Bay (Bouskill
281 et al., 2012; Hong et al., 2014) and they are capable of NO₂⁻ reduction to N₂O, whereas NO₃⁻ reduction to N₂O is solely
282 mediated by heterotrophic denitrifiers. N₂O production via nitrifier denitrification occurs under the full range of oxygen
283 environments in agricultural soil (Zhu et al., 2013) and the open ocean (Wilson et al., 2014). Partial denitrification (NO₃⁻
284 reduction to N₂O) however, is moderately oxygen sensitive. Thus, increasing oxygen inhibits the activities of denitrifiers, as
285 demonstrated in decreasing rates of NO₃⁻ reduction to N₂O (Fig. 3) and NO₃⁻ reduction to NO₂⁻ (Fig. 5). Increasing oxygen
286 does not completely inhibit N₂O production activity of nitrifiers but probably lowers the N₂O production rates by nitrifier
287 denitrification.

288 **4 Conclusion and outlook**

289 The Chesapeake Bay is a potential N₂O source via denitrification when NO₃⁻ and NO₂⁻ are present under anoxic
290 conditions. Relative rates of NO₃⁻ and NO₂⁻ reduction to N₂O were positively correlated with relative concentrations of NO₃⁻
291 and NO₂⁻. Increased oxygen either by natural water column oxygenation or by experimental manipulation, decreased N₂O
292 production rates via denitrification. The size of the denitrifying community increased with increasing rates of N₂O production
293 via denitrification. The potential N₂O production in the summertime suggests that intermittent N₂O efflux to the atmosphere
294 could occur when a shallow oxic-anoxic interface (typically 10 – 15 m) is present (Taft et al., 1980; Kemp et al., 1992; Lee et
295 al., 2015a), and frequent disturbance of water column stratification by storm events, boat traffic and surface cooling. The
296 seasonal variation of surface and water column N₂O saturation levels (air-undersaturated in May and air-oversaturated in
297 November), and the detection of significant N₂O production in July (summer) when N₂O concentrations were the lowest imply

298 that N₂O consumption was also occurring in the Chesapeake Bay and probably minimizing N₂O efflux to the atmosphere. A
299 long-term, comprehensive survey with wide spatial coverage will help assess if the Chesapeake Bay is a net N₂O source or
300 sink on an annual scale, and to investigate the physical, chemical and biological controls of N₂O emission in the Chesapeake
301 Bay.

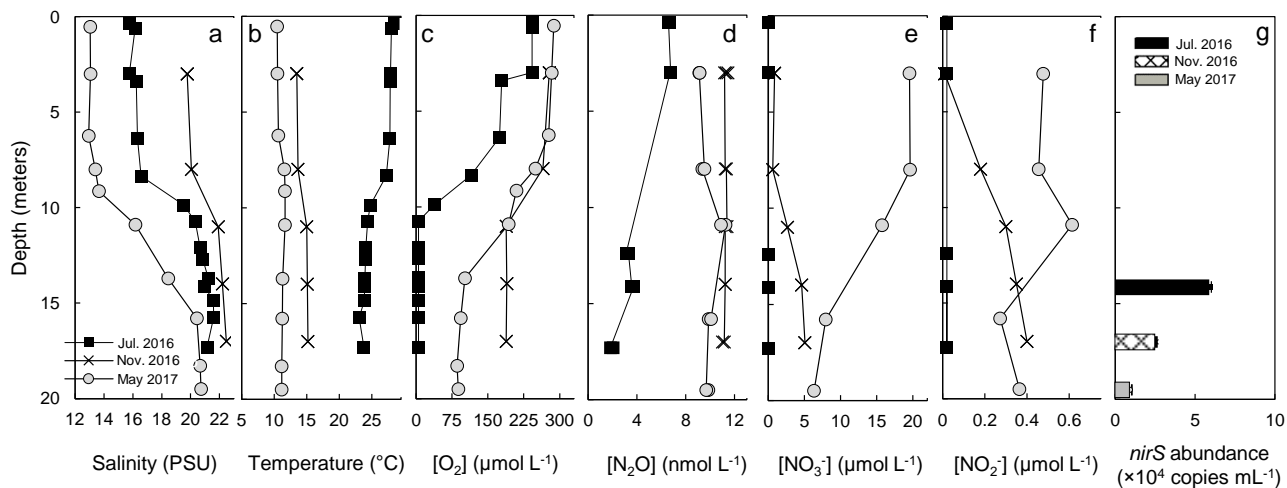
302 Denitrification is critical for complete removal of fixed nitrogen so as to mitigate eutrophication in natural waters. The
303 N₂O production rates could serve as a proxy for estimating nitrogen loss. It is estimated that 1% of total denitrified nitrogen is
304 converted to N₂O in river networks (Beaulieu et al., 2011) so the ratio of N₂O : N₂ during denitrification = 1 : 100. Assuming
305 that N₂O production occurs at a rate of 7 nmol-N L⁻¹ hr⁻¹ within 0.2 m of the oxic-anoxic interface in summertime (based on
306 the July 2016 control data, N₂O production from NO₃⁻ plus NO₂⁻), denitrification yields a potential water column nitrogen
307 removal rate of 140 μmol-N m⁻² hr⁻¹, or 0.24 mg-N m⁻² d⁻¹. In addition, the sediment in the Bay is capable of anaerobic ammonia
308 oxidation (Rich et al., 2008) and denitrification (Kemp et al., 1990; Kana et al., 2006). Total sedimentary N₂ production,
309 measured by the acetylene block reduction method (Kemp et al., 1990) and N₂ accumulation method (Kana et al., 2006)
310 recorded areal rates of 50 – 70 μmol-N m⁻² hr⁻¹. [Therefore, expansion of anoxia in the Chesapeake Bay could increase the
311 potential of biological nitrogen removal by the sediment-water system that counteracts the increase of nitrogen loading from
312 anthropogenic activities.](#)

313 The oxidation of NH₄⁺, although not the focus of this study, is a possible pathway for N₂O production under low oxygen
314 conditions (Anderson, 1964). The yield of N₂O (molar ratio of N₂O production to NH₄⁺ oxidation) increases with decreasing
315 oxygen (Goreau et al., 1980). Culture (Qin et al., 2017) and field studies (Bristow et al., 2016; Peng et al., 2016) have shown
316 high affinity of oxygen (< 5 μmol L⁻¹) during NH₄⁺ oxidation. The main sources of NH₄⁺ in the Chesapeake Bay include
317 remineralization of organic matter in the oxygenated water column and sediments (Kemp et al., 1990) and atmospheric
318 deposition (Larsen et al., 2001). Onset of NH₄⁺ oxidation is viable at NH₄⁺ concentration < 100 nmol L⁻¹ by the natural
319 ammonia oxidizing community (Horak et al., 2013). Thus, N₂O production from NH₄⁺ oxidation might be stimulated under
320 low oxygen condition by influx of ammonium near the oxic-anoxic interface, which deserves future research efforts.

321 The inhibition of N₂O production by oxygen highlights the positive outcomes of re-oxygenation of the Chesapeake Bay.
322 Since the late 20th century, Chesapeake Bay has received increased anthropogenic nitrogen loading from various sources

323 including fertilizer (Groffman et al., 2009), untreated sewage (Kaplan et al., 1978) and atmospheric deposition (Russell et al.,
324 1998; Loughner et al., 2016). Fueled by increased nitrogen input, elevated primary production in the surface layer stimulates
325 aerobic remineralization at depth, which consumes oxygen rapidly. In summertime, water column stratification restricts influx
326 of oxygen to depth, creating seasonal anoxia/hypoxia in the Bay. The documented eutrophication and expansion of
327 anoxia/hypoxia in the Chesapeake Bay in the late 20th century attracted public attention because of increasing mortality of
328 organisms with high commercial and recreational value (Cooper and Brush, 1993). Moreover, expansion of the volume of low
329 oxygen waters will result in more “hot spots” for N₂O production. The key factor of mitigating anoxia is to control the nitrogen
330 input to the bay (Hagy et al., 2004; Zhou et al., 2014). Effective fertilizer application, sewage treatment, natural nitrogen
331 removal by denitrification/anammox, and plant uptake have been successfully enforced to control the nitrogen runoff into the
332 bay from the tributaries (Boesch et al., 2001). The near absence of summertime water column NO₂⁻ + NO₃⁻ concentrations
333 close to the central Chesapeake Bay as shown in this study and others (Lee et al., 2015a) could prevent N₂O production.
334 Reducing the nitrogen input into the Chesapeake Bay will help mitigate N₂O efflux: In the short-term (time scale of days to
335 months), nitrogen sources (NH₄⁺, NO₂⁻ and NO₃⁻) for N₂O production will be decreased. In the long run (inter-annual time
336 scale), eutrophication will be alleviated, which will re-oxygenate the water column, and inhibit N₂O production.

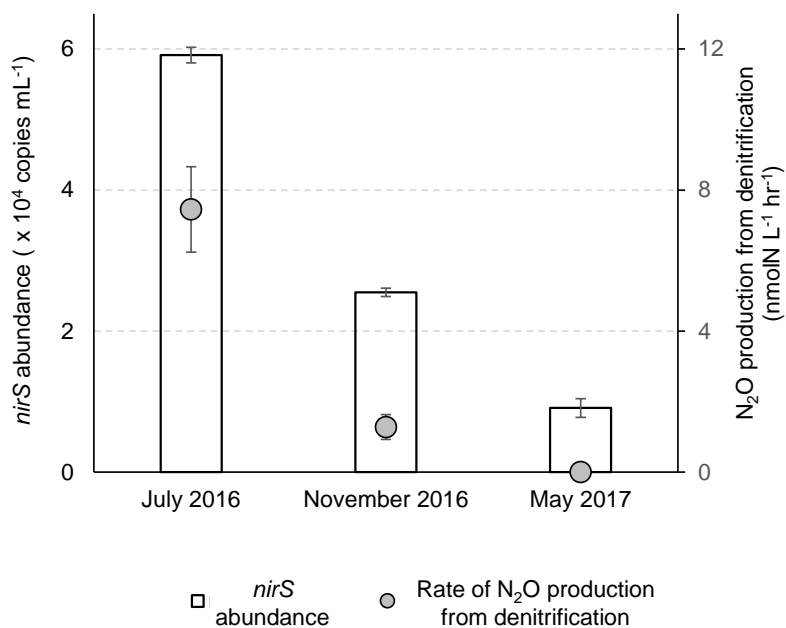
337



338

339 **Figure 1: Depth profiles on three sampling dates, July 19, 2016 (filled square), November 17, 2016 (cross), May 3, 2017 (grey circle)**
 340 **of a) salinity, b) temperature, c) oxygen, d) nitrous oxide, e) nitrate, f) nitrite. Analysis of *nirS* gene abundance (g) was only conducted**
 341 **at one depth, at which incubations were also performed, during each trip.**

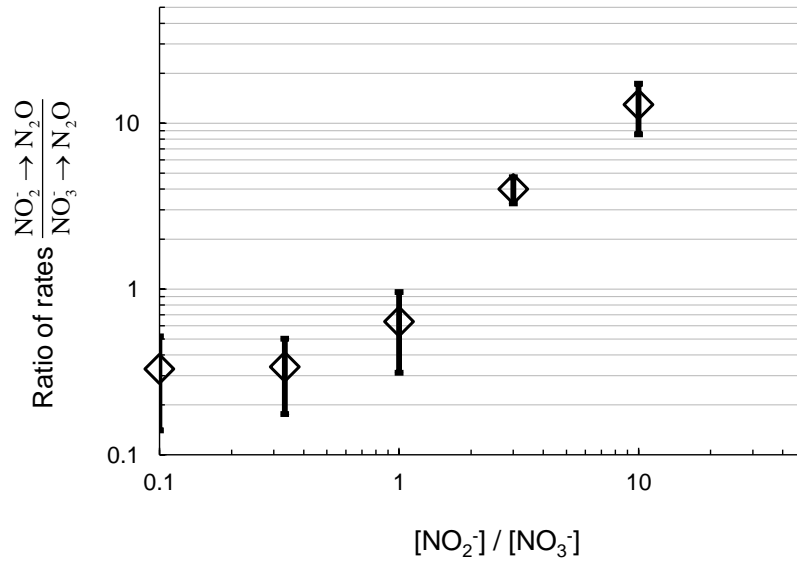
342



343

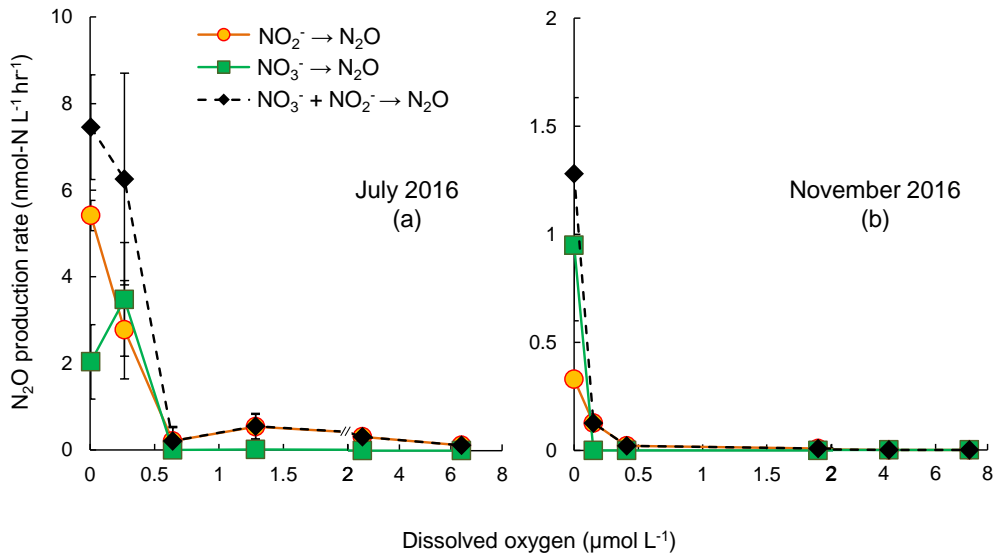
344 **Figure 2: Abundances of *nirS* gene and rates of N₂O production from nitrate plus nitrite reduction at three sampling times. The *nirS***
 345 **gene abundances were analyzed at 14.1, 17.0 and 19.5 m during July 2016, November 2016 and May 2017, respectively. The N₂O**
 346 **production rates were measured in the control experiment (helium-flushed anoxic incubation) at 12.3, 17.0 and 19.5 m during July**
 347 **2016, November 2016 and May 2017, respectively.**

348



350
351
352
353
354

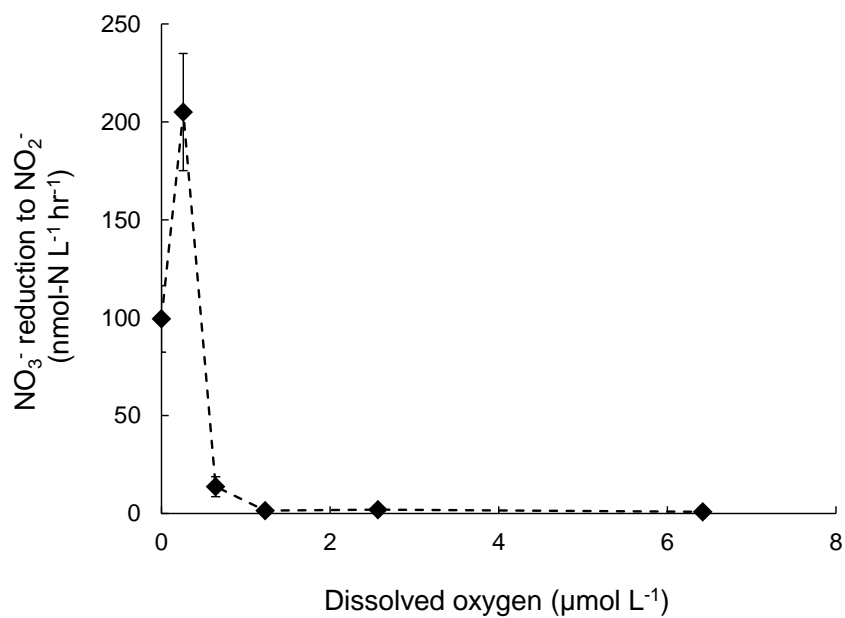
Figure 3: Ratio of rates of N₂O production from NO₂⁻ reduction and NO₃⁻ reduction plotted with the respective ratio of NO₂⁻ to NO₃⁻ concentration in the DIN manipulation experiment from July 2016 sampling. Log scale on both axes is for clarity at the low values.



355

Figure 4: Rates of N₂O production from NO₂⁻ reduction (orange circles), NO₃⁻ reduction (green squares) and combined NO₂⁻ and NO₃⁻ reduction (black diamonds) under increasing oxygen concentrations in July 2016 (a) and November 2016 (b). The standard deviation of rates in most of the samples were small so that error bars are not visible. Note the scale break at 2 µmol L⁻¹ O₂ on x-axis.

360
361



362 **Figure 5: Rates of NO₂⁻ production from NO₃⁻ reduction under increasing oxygen concentrations. Error bar indicates the standard**
363 **deviation of rates from linear regression of three time points (n=7).**
364

365

Experiment	Experiment ID	¹⁵ NO ₂ ⁻ (μM)	¹⁵ NO ₃ ⁻ (μM)	¹⁴ NO ₂ ⁻ (μM)	¹⁴ NO ₃ ⁻ (μM)	NO ₂ ⁻ :NO ₃ ⁻	¹⁵ N fraction label (species)	O ₂ (μM)
Control (July 2016)	1-A	5			5	1:1	0.99 (NO ₂ ⁻)	0
	1-B		5	5		1:1	0.99 (NO ₃ ⁻)	0
Nitrogen manipulation (July 2016)	2-A	0.2		1	10	1.2 : 10	0.16 (NO ₂ ⁻)	0
	2-B		0.2	1	10	1 : 10.2	0.016 (NO ₃ ⁻)	0
	2-C	0.2		1	3	1.2 : 3	0.16 (NO ₂ ⁻)	0
	2-D		0.2	1	3	1 : 3.2	0.06 (NO ₃ ⁻)	0
	2-E	0.2		3	1	3.2 : 1	0.06 (NO ₂ ⁻)	0
	2-F		0.2	3	1	3 : 1.2	0.16 (NO ₃ ⁻)	0
	2-G	0.2		10	1	10.2 : 1	0.016 (NO ₂ ⁻)	0
	2-H		0.2	10	1	10 : 1.2	0.16 (NO ₃ ⁻)	0
Oxygen manipulation (July 2016)	3-A	5			5	1:1	0.99 (NO ₂ ⁻)	0.3
	3-B		5	5		1:1	0.99 (NO ₃ ⁻)	0.3
	3-C	5			5	1:1	0.99 (NO ₂ ⁻)	0.6
	3-D		5	5		1:1	0.99 (NO ₃ ⁻)	0.6
	3-E	5			5	1:1	0.99 (NO ₂ ⁻)	1.3
	3-F		5	5		1:1	0.99 (NO ₃ ⁻)	1.3
	3-G	5			5	1:1	0.99 (NO ₂ ⁻)	2.6
	3-H		5	5		1:1	0.99 (NO ₃ ⁻)	2.6
	3-I	5			5	1:1	0.99 (NO ₂ ⁻)	6.4
	3-J		5	5		1:1	0.99 (NO ₃ ⁻)	6.4
Control (November 2016)	4-A	5		0.4	10	0.54:1	0.93 (NO ₂ ⁻)	0
	4-B		5	5.4	5	0.54:1	0.50 (NO ₃ ⁻)	0
Oxygen manipulation (November 2016)	5-A	5		0.4	10	0.54:1	0.93 (NO ₂ ⁻)	0.2
	5-B		5	5.4	5	0.54:1	0.50 (NO ₃ ⁻)	0.2
	5-C	5		0.4	10	0.54:1	0.93 (NO ₂ ⁻)	0.4
	5-D		5	5.4	5	0.54:1	0.50 (NO ₃ ⁻)	0.4
	5-E	5		0.4	10	0.54:1	0.93 (NO ₂ ⁻)	1.9
	5-F		5	5.4	5	0.54:1	0.50 (NO ₃ ⁻)	1.9
	5-G	5		0.4	10	0.54:1	0.93 (NO ₂ ⁻)	4.2
	5-H		5	5.4	5	0.54:1	0.50 (NO ₃ ⁻)	4.2
	5-I	5		0.4	10	0.54:1	0.93 (NO ₂ ⁻)	7.3
	5-J		5	5.4	5	0.54:1	0.50 (NO ₃ ⁻)	7.3
Control (May 2017)	6-A	5		0.4	11.3	0.48:1	0.93 (NO ₂ ⁻)	0
	6-B		5	5.4	6.3	0.48:1	0.44 (NO ₃ ⁻)	0

366

367 **Table 1: Parameters for control, nitrogen manipulation and oxygen manipulation incubation experiments in July 2016, November**
368 **2016 and May 2017 sampling. In May 2017, only control experiment was conducted. The unit “μmol L⁻¹” is represented by “μM”.**
369 **Shaded columns highlight the concentrations for ¹⁵N tracers. In situ nitrate and nitrite concentrations in July 2016 were < 0.02**
370 **μmol L⁻¹; in November 2016 the concentrations were 5.0 and 0.4 μmol L⁻¹, respectively; in May 2017 the concentrations were 6.3**
371 **and 0.4 μmol L⁻¹, respectively.**

372
373
374

375 **5 Funding Sources and Acknowledgements**

376 This work is supported by the following funding sources: The PEI Grand Challenges – Control of Microbial Nitrous Oxide
377 Production in Coastal Waters to B.B.W.. National Science Foundation (OCE 1427019) to J.C.C.. German Academic Exchange
378 Service Postdoctoral Researchers International Mobility Experience fellowship to C.F. The authors would like to thank
379 Michael Owens at Horn Point Laboratory for his assistance with field research equipment. We thank Sergey Oleynik for
380 technical assistance during laboratory analysis.

381 **6 References**

- 382 Anderson, J. H.: The metabolism of hydroxylamine to nitrite by *Nitrosomonas*, *Biochem. J.*, 91, 8-17, 1964.
383
384 Arp, D. J., and Stein, L. Y.: Metabolism of inorganic N compounds by ammonia-oxidizing bacteria, *Crit Rev Biochem Mol Biol*, 38, 471-
385 495, doi:10.1080/10409230390267446, 2003.
386
387 Baird, D., Ulanowicz, R. E., and Boynton, W. R.: Seasonal Nitrogen Dynamics in Chesapeake Bay: a Network Approach, *Estuar. Coast.*
388 *Shelf Sci.*, 41, 137-162, doi:10.1006/ecss.1995.0058, 1995.
389
390 Beaulieu, J. J., Tank, J. L., Hamilton, S. K., Wollheim, W. M., Hall, R. O., Mulholland, P. J., Peterson, B. J., Ashkenas, L. R., Cooper, L.
391 W., Dahm, C. N., Dodds, W. K., Grimm, N. B., Johnson, S. L., McDowell, W. H., Poole, G. C., Valett, H. M., Arango, C. P., Bernot, M. J.,
392 Burgin, A. J., Crenshaw, C. L., Helton, A. M., Johnson, L. T., O'Brien, J. M., Potter, J. D., Sheibley, R. W., Sobota, D. J., and Thomas, S.
393 M.: Nitrous oxide emission from denitrification in stream and river networks, *Proc. Natl. Acad. Sci. U.S.A.*, 108, 214-219,
394 doi:10.1073/pnas.1011464108, 2011.
395
396 Boesch, D. F., Brinsfield, R. B., and Magnien, R. E.: Chesapeake Bay Eutrophication, *J. Environ. Qual.*, 30, 303-320,
397 doi:10.2134/jeq2001.302303x, 2001.
398
399 Bouskill, N. J., Eveillard, D., Chien, D., Jayakumar, A., and Ward, B. B.: Environmental factors determining ammonia-oxidizing organism
400 distribution and diversity in marine environments, *Environ. Microbiol.*, 14, 714-729, doi:10.1111/j.1462-2920.2011.02623.x, 2012.
401
402 Boynton, W. R., Garber, J. H., Summers, R., and Kemp, W. M.: Inputs, transformations, and transport of nitrogen and phosphorus in
403 Chesapeake Bay and selected tributaries, *Estuaries*, 18, 285-314, doi:10.2307/1352640, 1995.
404
405 Braman, R. S., and Hendrix, S. A.: Nanogram nitrite and nitrate determination in environmental and biological materials by vanadium(III)
406 reduction with chemiluminescence detection, *Anal. Chem.*, 61, 2715-2718, doi:10.1021/ac00199a007, 1989.
407
408 Bristow, L. A., Dalsgaard, T., Tiano, L., Mills, D. B., Bertagnolli, A. D., Wright, J. J., Hallam, S. J., Ulloa, O., Canfield, D. E., and Revsbech,
409 N. P.: Ammonium and nitrite oxidation at nanomolar oxygen concentrations in oxygen minimum zone waters, *Proc. Natl. Acad. Sci. U.S.A.*,
410 113, 10601-10606, doi:10.1073/pnas.1600359113, 2016.
411
412 Ciais, P., C. Sabine, G. Bala, L. Bopp, V. Brovkin, J. Canadell, A. Chhabra, R. DeFries, J. Galloway, M. Heimann, C. Jones, C. Le Quéré
413 R.B. Myneni, Piao, S., and Thornton, P.: Carbon and Other Biogeochemical Cycles, Cambridge, United Kingdom and New York, NY, USA,
414 465-570, 2013.
415
416 Cooper, S. R., and Brush, G. S.: A 2,500-Year History of Anoxia and Eutrophication in Chesapeake Bay, *Estuaries*, 16, 617-626,
417 doi:10.2307/1352799, 1993.
418

419 Dürr, H. H., Laruelle, G. G., van Kempen, C. M., Slomp, C. P., Meybeck, M., and Middelkoop, H.: Worldwide Typology of Nearshore
420 Coastal Systems: Defining the Estuarine Filter of River Inputs to the Oceans, *Estuaries Coasts*, 34, 441-458, doi:10.1007/s12237-011-9381-
421 y, 2011.

422

423 Eggleston, E. M., Lee, D. Y., Owens, M. S., Cornwell, J. C., Crump, B. C., and Hewson, I.: Key respiratory genes elucidate bacterial
424 community respiration in a seasonally anoxic estuary, *Environ. Microbiol.*, 17, 2306-2318, doi:10.1111/1462-2920.12690, 2015.

425

426 Elkins, J. W., Steven C. Wofsy, Michael B. McElroy, Charles E. Kolb, and Kaplan, W. A.: Aquatic sources and sinks for nitrous oxide,
427 *Nature*, 275, 602-606, doi:10.1038/275602a0, 1978.

428

429 Frame, C. H., and Casciotti, K. L.: Biogeochemical controls and isotopic signatures of nitrous oxide production by a marine ammonia-
430 oxidizing bacterium, *Biogeosciences*, 7, 2695-2709, doi:10.5194/bg-7-2695-2010, 2010.

431

432 Garcia, H. E., and Gordon, L. I.: Oxygen solubility in seawater: Better fitting equations, *Limnol. Oceanogr.*, 37, 1307-1312,
433 doi:10.4319/lo.1992.37.6.1307, 1992.

434

435 Garside, C.: A chemiluminescent technique for the determination of nanomolar concentrations of nitrate and nitrite in seawater, *Mar. Chem.*,
436 11, 159-167, doi:10.1016/0304-4203(82)90039-1, 1982.

437

438 Goreau, T. J., Kaplan, W. A., Wofsy, S. C., McElroy, M. B., Valois, F. W., and Watson, S. W.: Production of NO₂⁻ and N₂O by nitrifying
439 bacteria at reduced concentrations of oxygen, *Appl. Environ. Microbiol.*, 40, 526-532, 1980.

440

441 Graf, D. R. H., Jones, C. M., and Hallin, S.: Intergenomic Comparisons Highlight Modularity of the Denitrification Pathway and Underpin
442 the Importance of Community Structure for N₂O Emissions, *PLOS ONE*, 9, e114118, doi:10.1371/journal.pone.0114118, 2014.

443

444 Groffman, P. M., Williams, C. O., Pouyat, R. V., Band, L. E., and Yesilonis, I. D.: Nitrate leaching and nitrous oxide flux in urban forests
445 and grasslands, *J. Environ. Qual.*, 38, 1848-1860, doi:10.2134/jeq2008.0521, 2009.

446

447 Hagy, J. D., Boynton, W. R., Keefe, C. W., and Wood, K. V.: Hypoxia in Chesapeake Bay, 1950–2001: Long-term change in relation to
448 nutrient loading and river flow, *Estuaries*, 27, 634-658, doi:10.1007/BF02907650, 2004.

449

450 Hansen, H. P., and Koroleff, F.: Determination of nutrients, in: *Methods of Seawater Analysis*, Wiley-VCH Verlag GmbH, 159-228, 2007.

451

452 Hong, Y., Xu, X., Kan, J., and Chen, F.: Linking seasonal inorganic nitrogen shift to the dynamics of microbial communities in the
453 Chesapeake Bay, *Appl Microbiol Biotechnol*, 98, 3219, doi:10.1007/s00253-013-5337-4, 2014.

454

455 Horak, R. E. A., Qin, W., Schauer, A. J., Armbrust, E. V., Ingalls, A. E., Moffett, J. W., Stahl, D. A., and Devol, A. H.: Ammonia oxidation
456 kinetics and temperature sensitivity of a natural marine community dominated by Archaea, *ISME J*, 7, 2023-2033,
457 doi:10.1038/ismej.2013.75, 2013.

458

459 Jayakumar, A., O'Mullan, G. D., Naqvi, S. W. A., and Ward, B. B.: Denitrifying Bacterial Community Composition Changes Associated
460 with Stages of Denitrification in Oxygen Minimum Zones, *Microb. Ecol.*, 58, 350-362, doi:10.1007/s00248-009-9487-y, 2009.

461

462 Jayakumar, A., Peng, X., and Ward, B. B.: Community composition of bacteria involved in fixed nitrogen loss in the water column of two
463 major oxygen minimum zones in the ocean, *Aquatic Microbial Ecology*, 70, 245-259, doi:10.3354/ame01654, 2013.

464

465 Kana, T. M., Cornwell, J. C., and Zhong, L.: Determination of Denitrification in the Chesapeake Bay from Measurements of N₂^₂
466 Accumulation in Bottom Water, *Estuaries Coasts*, 29, 222-231, 2006.

467

468 Kaplan, W. A., Elkins, J. W., Kolb, C. E., McElroy, M. B., Wofsy, S. C., and Durán, A. P.: Nitrous oxide in fresh water systems: An estimate
469 for the yield of atmospheric N₂O associated with disposal of human waste, *Pure Appl. Geophys.*, 116, 423-438, doi:10.1007/bf01636897,
470 1978.

471

472 Kartal, B., Maalcke, W. J., de Almeida, N. M., Cirpus, I., Gloerich, J., Geerts, W., Op den Camp, H. J. M., Harhangi, H. R., Janssen-Megens,
473 E. M., Francoijs, K.-J., Stunnenberg, H. G., Keltjens, J. T., Jetten, M. S. M., and Strous, M.: Molecular mechanism of anaerobic ammonium
474 oxidation, *Nature*, 479, 127-130, doi:10.1038/nature10453, 2011.

475
476 Kemp, W., Sampou, P., Caffrey, J., Mayer, M., Henriksen, K., and Boynton, W. R.: Ammonium recycling versus denitrification in
477 Chesapeake Bay sediments, *Limnol. Oceanogr.*, 35, 1545-1563, 1990.
478
479 Kemp, W. M., Sampou, P. A., Garber, J., Tuttle, J., and Boynton, W. R.: Seasonal depletion of oxygen from bottom waters of Chesapeake
480 Bay: roles of benthic and planktonic respiration and physical exchange processes, *Mar. Ecol. Prog. Ser.*, 85, 137-152, 1992.
481
482 Larsen, R. K., Steinbacher, J. C., and Baker, J. E.: Ammonia exchange between the atmosphere and the surface waters at two locations in
483 the Chesapeake Bay, *Environ. Sci. Technol.*, 35, 4731-4738, doi:10.1021/es0107551, 2001.
484
485 Lee, D. Y., Owens, M. S., Crump, B. C., and Cornwell, J. C.: Elevated microbial CO₂ production and fixation in the oxic/anoxic interface
486 of estuarine water columns during seasonal anoxia, *Estuar. Coast. Shelf Sci.*, 164, 65-76, doi:10.1016/j.ecss.2015.07.015, 2015a.
487
488 Lee, D. Y., Owens, M. S., Doherty, M., Eggleston, E. M., Hewson, I., Crump, B. C., and Cornwell, J. C.: The Effects of Oxygen Transition
489 on Community Respiration and Potential Chemoautotrophic Production in a Seasonally Stratified Anoxic Estuary, *Estuaries Coasts*, 38, 104-
490 117, doi:10.1007/s12237-014-9803-8, 2015b.
491
492 Loughner, C. P., Tzortziou, M., Shroder, S., and Pickering, K. E.: Enhanced dry deposition of nitrogen pollution near coastlines: A case
493 study covering the Chesapeake Bay estuary and Atlantic Ocean coastline, *J. Geophys. Res.: Atmos.*, 121, 14,221-214,238,
494 doi:10.1002/2016JD025571, 2016.
495
496 McElroy, M. B., Elkins, J. W., Wofsy, S. C., Kolb, C. E., Durán, A. P., and Kaplan, W. A.: Production and release of N₂O from the Potomac
497 Estuary 1, *Limnol. Oceanogr.*, 23, 1168-1182, doi:10.4319/lo.1978.23.6.1168, 1978.
498
499 McIlvin, M. R., and Altabet, M. A.: Chemical conversion of nitrate and nitrite to nitrous oxide for nitrogen and oxygen isotopic analysis in
500 freshwater and seawater, *Anal. Chem.*, 77, 5589-5595, doi:10.1021/ac050528s, 2005.
501
502 Moir, J. W. B., and Wood, N. J.: Nitrate and nitrite transport in bacteria, *Cell. Mol. Life Sci.*, 58, 215-224, doi:10.1007/PL00000849, 2001.
503
504 Peng, X., Fuchsman, C. A., Jayakumar, A., Warner, M. J., Devol, A. H., and Ward, B. B.: Revisiting nitrification in the Eastern Tropical
505 South Pacific: A focus on controls, *J. Geophys. Res.: Oceans*, 121, 1667-1684, doi:10.1002/2015JC011455, 2016.
506
507 Poth, M., and Focht, D. D.: (15)N Kinetic Analysis of N(2)O Production by *Nitrosomonas europaea*: an Examination of Nitrifier
508 Denitrification, *Appl. Environ. Microbiol.*, 49, 1134-1141, 1985.
509
510 Qin, W., Meinhardt, K. A., Moffett, J. W., Devol, A. H., Virginia Armbrust, E., Ingalls, A. E., and Stahl, D. A.: Influence of oxygen
511 availability on the activities of ammonia-oxidizing archaea, *Environ. Microbiol. Rep.*, 9, 250-256, doi:10.1111/1758-2229.12525, 2017.
512
513 Ravishankara, A., Daniel, J. S., and Portmann, R. W.: Nitrous oxide (N₂O): the dominant ozone-depleting substance emitted in the 21st
514 century, *Science*, 326, 123-125, 2009.
515
516 Rich, J. J., Dale, O. R., Song, B., and Ward, B. B.: Anaerobic ammonium oxidation (anammox) in Chesapeake Bay sediments, *Microb.*
517 *Ecol.*, 55, 311-320, doi:10.1007/s00248-007-9277-3, 2008.
518
519 Russell, K. M., Galloway, J. N., Macko, S. A., Moody, J. L., and Scudlark, J. R.: Sources of nitrogen in wet deposition to the Chesapeake
520 Bay region, *Atmos. Environ.*, 32, 2453-2465, doi:10.1016/S1352-2310(98)00044-2, 1998.
521
522 Santoro, A. E., Buchwald, C., McIlvin, M. R., and Casciotti, K. L.: Isotopic Signature of N₂O Produced by Marine Ammonia-Oxidizing
523 Archaea, *Science*, 333, 1282-1285, doi:10.1126/science.1208239, 2011.
524
525 Schilt, A., Baumgartner, M., Blunier, T., Schwander, J., Spahni, R., Fischer, H., and Stocker, T. F.: Glacial–interglacial and millennial-scale
526 variations in the atmospheric nitrous oxide concentration during the last 800,000 years, *Quat. Sci. Rev.*, 29, 182-192,
527 doi:10.1016/j.quascirev.2009.03.011, 2010.
528
529 Seitzinger, S. P., and Kroeze, C.: Global distribution of nitrous oxide production and N inputs in freshwater and coastal marine ecosystems,
530 *Glob. Biogeochem. Cycles*, 12, 93-113, doi:10.1029/97GB03657, 1998.

531
532 Taft, J. L., Taylor, W. R., Hartwig, E. O., and Loftus, R.: Seasonal oxygen depletion in Chesapeake Bay, *Estuaries*, 3, 242-247,
533 doi:10.2307/1352079, 1980.
534
535 Thompson, R. L., Chevallier, F., Crotwell, A. M., Dutton, G., Langenfelds, R. L., Prinn, R. G., Weiss, R. F., Tohjima, Y., Nakazawa, T.,
536 Krummel, P. B., Steele, L. P., Fraser, P., O'Doherty, S., Ishijima, K., and Aoki, S.: Nitrous oxide emissions 1999 to 2009 from a global
537 atmospheric inversion, *Atmos. Chem. Phys.*, 14, 1801-1817, doi:10.5194/acp-14-1801-2014, 2014.
538
539 Weigand, M. A., Foriel, J., Barnett, B., Oleynik, S., and Sigman, D. M.: Updates to instrumentation and protocols for isotopic analysis of
540 nitrate by the denitrifier method, *Rapid Commun. Mass Spectrom.*, 30, 1365-1383, doi:10.1002/rcm.7570, 2016.
541
542 Weiss, R. F., and Price, B. A.: Nitrous oxide solubility in water and seawater, *Mar. Chem.*, 8, 347-359, doi:10.1016/0304-4203(80)90024-
543 9, 1980.
544
545 Wilson, S. T., del Valle, D. A., Segura-Noguera, M., and Karl, D. M.: A role for nitrite in the production of nitrous oxide in the lower
546 euphotic zone of the oligotrophic North Pacific Ocean, *Deep-Sea Res. I*, 85, 47-55, doi:10.1016/j.dsr.2013.11.008, 2014.
547
548 Zhou, Y., Scavia, D., and Michalak, A. M.: Nutrient loading and meteorological conditions explain interannual variability of hypoxia in
549 Chesapeake Bay, *Limnol. Oceanogr.*, 59, 373-384, doi:10.4319/lo.2014.59.2.0373, 2014.
550
551 Zhu, X., Burger, M., Doane, T. A., and Horwath, W. R.: Ammonia oxidation pathways and nitrifier denitrification are significant sources of
552 N₂O and NO under low oxygen availability, *Proc. Natl. Acad. Sci. U.S.A.*, 110, 6328-6333, doi:10.1073/pnas.1219993110, 2013.